Chemical Engineering Journal 188 (2012) 160–172

Contents lists available at SciVerse ScienceDirect

Chemical Engineering Journal

journal homepage: www.elsevier.com/locate/cej

A comparative study of epoxy resin cured with a linear diamine and a branched polyamine

Jintao Wan[a,b], Cheng Li[a], Zhi-Yang Bu[a], Cun-Jin Xu[c], Bo-Geng Li[a,*], Hong Fan[a,**]

[a] State Key Laboratory of Chemical Engineering, Department of Chemical and Biochemical Engineering, Zhejiang University, Hangzhou 310027, China
[b] Zhejiang Jiamin Plastics Company Ltd., Jiaxing 314027, China
[c] College of Material, Chemistry and Chemical Engineering, Hangzhou Normal University, Hangzhou 310036, China

ARTICLE INFO

Article history:
Received 12 September 2011
Received in revised form 31 January 2012
Accepted 31 January 2012

Keywords:
Epoxy resin
Curing agent
Branched polyamine
Model-fitting kinetics
Isoconversional kinetic analysis
Thermal properties

ABSTRACT

The molecular topology of amine curing agents is expected to greatly affect the curing reaction and properties of the epoxy resins, yet the exact influence still remains little understood. Herein we find out two representative aliphatic amines: linear propanediamine (PDA) and branched *N*,*N*,*N*′,*N*′-tetra(3-aminopropyl)-1,3-propanediamine (TAPA), and use them to cure diglycidyl ether of bisphenol A (DGEBA). The curing reaction, dynamic mechanical properties, and thermal stability of DGEBA/PDA and DGEBA/TAPA are systematically investigated and compared. Differential scanning calorimetry (DSC) confirms TAPA and PDA have very close reactivity much higher than that of commercial Jeffamine T-403 with the branched molecular structure. The curing kinetic analysis shows TAPA causes the higher isothermal conversion at the lower temperature (e.g., 40 °C), the autocatalysis and diffusion-associated kinetics feature the isothermal reactions, and the extended Kamal model turns out to be able to well predict the curing rate. Then, the isoconversional analysis with the Vyazovkin methods demonstrates compared to PDA, TAPA leads to the lower effective activation energy at the very beginning due to its catalytic tertiary amino groups, but the reversed trend emerges in the deep-conversion stage, especially, in the glass-transition regime, owing to its flexible aliphatic molecular chains. Furthermore, the isothermal conversion at the higher temperatures is predicted from the nonisothermal experiments. Finally, dynamic mechanical analysis (DMA) shows cured DGEBA/TAPA exhibits the higher glass- and β-relaxation temperatures and crosslink density than DGEBA/PDA, and thermogravimetric analysis (TGA) reveals TAPA-cured epoxy has the excellent thermal stability with the higher char yield.

1. Introduction

Epoxy resins find many important applications in protective coatings, adhesives, electronic-packaging materials, high-performance composites, etc., due to the high stiffness, dimension stability, mechanical strength, chemical and environment resistance, versatile processability, and favorable performance-cost ratio. In practical applications, a curing process is needed to transform epoxy resins from monomers or oligmers to a permanently highly crosslinked macromolecule in the presence of a curing agent via an epoxy ring-opening mechanism. Of all known and widely used curing agents, the amine-based ones are of primary importance. In particular, aliphatic amines have the advantages of high reactivity, low viscosity, melting temperatures, and wide availability, accounting for their major use in high-performance room-temperature-cure coatings and adhesives. However, the high volatility, strong sensitization, quick carbonatation in air, and very strict stoichiometry relative to epoxy resins limit their further applications, and the related healthy and safety considerations arise. To date, most attention is paid to the conventionally linear aliphatic amine curing agents, but nonlinear amines are still less addressed. On the other hand, a number of nonlinear multi-functional epoxy resins, e.g., *N*,*N*,*N*′,*N*′-tetraglycidyl-4,4′-diaminodiphenylmethane (TGDDM) [1] and triglycidyl amino phenyl (TGAP) [2], have received considerable interest, because of their lower viscosity, better flowability, processability, and outstanding thermo-mechanical performances compared to conventional linear bisphenol-A type epoxy resins (DGEBA). Moreover, recently a few attempts have being made to develop even more branched epoxy resins, i.e., hyperbranched epoxy resins with extraordinary high functionalities [3–6].

By analog, we can perceive that introducing the branched topology into the aliphatic amine molecules will probably result in some unusual properties. For example, branched aliphatic amines can

* Corresponding author. Tel.: +86 571 87952623; fax: +86 571 87951612.
** Corresponding author. Tel.: +86 571 87957371; fax: +86 571 87951612.
E-mail addresses: wan_jintao@yahoo.com.cn (J. Wan), bgli@zju.edu.cn (B.-G. Li), hfan@zju.edu.cn (H. Fan).

1385-8947/$ – see front matter © 2012 Elsevier B.V. All rights reserved.
doi:10.1016/j.cej.2012.01.134

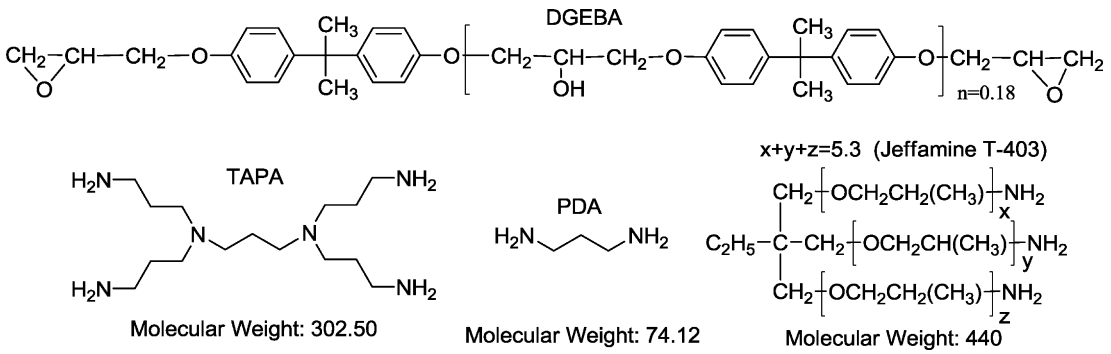

Scheme 1. Molecular structure of DGEBA, TAPA, PDA and Jeffamine T-403.

likely fulfill the demanding combination of the high functionalities, reactivity, crosslink density, low viscosity, volatility, slow carbonatation rate, and reduced crystallizability compared with their linear counterparts of close molecular weights [7]. A case in point is commercial Jeffamine T-403 [8–11] (Scheme 1) with the high functionalities, low volatility, excellent processability, light color, and retarded absorption of CO_2, and, more important, it can increase the high flexibility and toughness of the cured epoxy. Jeffamine T-403, however, is much less reactive than conventional aliphatic amines (e.g., ethanediamine, propanediamine, triethylenediamine, etc.) due to its primary amino groups linked to the bulky substituent, creating the high steric hindrance (NH_2—$CH(CH_3)$R). Also, Jeffamine T-403 has the rather high amino hydrogen equivalent weight (73.3 g/mol N—H) toward epoxy resins, which will significantly increase the application cost. Furthermore, Jeffamine T-403-cured epoxy resins still suffer from the lower glass temperatures and inferior solvent and water resistance compared to conventional aliphatic amines. These shortcomings restrict its further applications in the epoxy formulations where the fast cure, quick dry, thermal properties, and solvent and water resistance are especially important [12].

To meet this challenge, our recent studies [7,12–15] have demonstrated that it is a feasible way of achieving the desired properties of the epoxy resin by merely shifting the molecular architecture of the aliphatic amines from linear to nonlinear without introducing other kinds of elements like oxygen present in the Jeffamine T-403 molecules and increasing steric hindrance of the primary amino groups. In this regard, the molecular topology of such amine curing agents greatly affects the curing reaction and final properties of the cured epoxy; nevertheless, to date the exact influence is far away from being well understood. Such knowledge is especially important for better designing and further exploring the nonlinear aliphatic amine curing agents with highly sophisticated properties.

Here we select the two model aliphatic amines (Scheme 1) to cure DGEBA: linear 1,3-diaminopropane (PDA) and branched *N*,*N*,*N*′,*N*′-tetra(3-aminopropyl)-1,3-ethylenediamine (TAPA), and originally investigate the curing reaction, dynamic mechanical properties, and thermal decomposition in a comparative way. As can be found, PDA and TAPA contain the same kind of elements (C, N and H), but possess the distinctly varied topologies (linear vs. branched), and TAPA has the much higher molecular weight than PDA, significantly decreasing the volatility and moderately extending the stoichiometry with respect to epoxy resins. Moreover, the raw materials of TAPA are simple, less expensive propylenediamine, acrylonitrile and hydrogen, and its preparation conditions are not demanding. Furthermore, TAPA has the amino equivalent weight of 36.1 g/mol N—H, only about the half of Jeffamine T-403 (73.3 g/mol N—H), which will appreciably decrease the application cost. These advantages will favor the potential industrial scaling up and applications of TAPA. Our present contribution will not only disclose the effect of molecular topology of TAPA and PDA on the epoxy cure from the reaction kinetic perspective, but clarify the properties of the cured epoxy from the dynamic mechanical and thermogravimetric analysis as well.

2. Experimental

2.1. Materials

Propylenediamine (PDA, 99%, Acros organics, USA) was used as received, and Jeffamine T-403, trimethylolpropane tris[poly(propylene glycol), amine terminated] ether, with the number averaged molecular weight of 440 Da was purchased from Sigma–Aldrich Co. Acrylonitrile (+98%) was obtained from Shanghai Reagent Co., and purified by distillation before use. The epoxy resins, diglycidyl ether of bisphenol A (DGEBA, Heli Resin Co., China) with the epoxide equivalent weight (EEW) of 196 g/equiv. was desiccated in vacuum before use. *N*,*N*,*N*′,*N*′-tetra(3-aminopropyl)-1,3-propylenediamine (TAPA) was synthesized by reacting PDA with excessive acrylonitrile according to the Michael addition mechanism, followed by the heterogeneously catalyzed hydrogenation with reference to published procedures [13,16,17]. The ^{1}H NMR spectrum of TAPA is presented as the supplementary material; see Appendix. TAPA: ^{1}H NMR (400 MHz, in $CDCl_3$) δ ppm 1.29, s, 8H, $N\underline{H}_2$; 1.57, m, 10H, $CH_2C\underline{H}_2CH_2$; 2.39, t, $NC\underline{H}_2CH_2C\underline{H}_2N$, 4H; 2.44, t, 8H, $NC\underline{H}_2CH_2CH_2NH_2$; 2.71, t, 8H, $C\underline{H}_2NH_2$. Other reagents and solvents were used as received.

2.2. Differential scanning calorimetry (DSC)

All the isothermal and nonisothermal experiments related to DGEBA/TAPA and DGEBA/PDA were preformed on a differential scanning calorimeter (DSC, Perkin Elemer-7, USA) calibrated with the In standard, while all the nonisothermal experiments bearing on DGEBA/Jeffamine T-403 were carried out on a NETZSCH DSC (DSC 200 F3, Germany) with an inter cooler (IC40) calibrated with the Hg, In, Zn, Sn and Bi standards. Stoichiometric DGEBA and the curing agent (TAPA, PDA, or Jeffamine T-403) were quickly mixed well (<5 min) at room temperature (<15 °C), and immediately the mixture (10 ± 2 mg) was enclosed in an aluminum crucibles to be subjected to the DSC measurement with an identical crucible as the reference. For the isothermal experiments, the sample was promptly heated to 40, 50, 60 or 70 °C with 100 °C/min to start and finish the isothermal run, followed by a second heating from 25 to 250 °C with 10 °C/min to measure the residual reaction enthalpy. To examine the reactivity of these amines, a dynamic DSC run was conducted on these epoxy-amine systems with the same heating rate of 5 °C/min from 25 to 250 °C. Moreover, the multi-heating rate experiments were conducted on DGEBA/TAPA and DGEBA/PDA with 5, 10, 15 and 20 °C/min. In addition, the glass temperatures of the fully

cured epoxy ($T_{g\infty}$S) were determined from a dynamic heating from well blow $T_{g\infty}$ to 200 °C with 10 °C/min.

2.3. Dynamic mechanical analysis (DMA)

Stoichiometric DGEBA and TAPA or PDA were mixed well at room temperature, and then poured into a preheated (40 °C) stainless-steel mould. Then, the mould was placed into a oven under reduced pressure to drive off any entrapped bubbles, and transferred to air-blast oven and heated to 70 °C for 1.5 h and subsequent at 150 °C for another 2.5 h. After demoduling, the cured casting epoxy bars (35 mm × 10 mm × 2 mm) were obtained and subjected to the subsequent thermo-mechanical analysis using a dynamic mechanical analyzer (DMA Q800, TA Instruments, USA). The specimen was fixed on a single cantilever clip, the heating rate was 3 °C/min, the oscillation frequency was 1 Hz, and the displacement was fixed at 15 μm. The temperature ranged from −100 °C to well above the glass temperature.

2.4. Thermogravimetric analysis (TGA)

The thermal decomposition of cured DGEBA/TAPA and DGEBA/PDA was examined using a thermogravimetric analyzer (Pyris 1 TGA, USA) with the heating rate of 10 °C/min from 40 to 850 °C under the N_2 protection (40 ml/min). About 2 mg of the cured epoxy was charged in a mica crucible without a lid.

3. Fundamental of curing kinetics

Curing reactions of epoxy resins are a high exothermic process, whose kinetic issues are most frequently studied with a DSC technique in isothermal and/or nonisothermal modes. In this case, the registered DSC heat flow characterizing the reaction exothermic rate is directly proportional to the reaction rate, and thus the fractional conversion of epoxy groups, α, can be written as

$$\alpha = \frac{\int_0^t H\,dt}{\int_0^{t_f} H\,dt} \tag{1}$$

where H is the heat flow, t is the reaction time, and t_f is completion time of the reaction.

Two methodologies are most frequently applied to kinetic studies of curing reactions: the model-fitting and model-free isoconversional ones. The former need select a reaction model with which to fit experimental kinetic rate to estimate the model parameters to establish a rate equation. For isothermal cure, the most frequently utilized models are the nth-order model, Eq. (2), [18] and the autocatalytic Kamal model, Eq. (3), [19,20].

$$\frac{d\alpha}{dt} = k(T)(1-\alpha)^n \tag{2}$$

$$\frac{d\alpha}{dt} = [k_1(T) + k_2(T)\alpha^m](1-\alpha)^n \tag{3}$$

In these two models, $k(T)$ is the temperature-dependent reaction rate constant, $k_1(T)$ is the non-autocatalytic rate constant corresponding to the initial reaction rate constant, $k_2(T)$ is the autocatalytic reaction rate constant associated with the catalytic species formed during the cure, and m and n are the orders of the non-autocatalytic and autocatalytic reactions, respectively. All the rate constants follow the Arrhenius equation:

$$k = A\exp\left(\frac{-E_a}{RT}\right) \tag{4}$$

As far as the model-free isoconversional methodologies are concerned, they are built upon the isoconversional principle stating that the reaction rate at constant extent of conversion is only a function of the temperature:

$$\left[\frac{d\ln(d\alpha/dt)}{dT^{-1}}\right]_\alpha = -\frac{E_\alpha}{R} \tag{5}$$

From Eq. (5), the temperature dependence of the isoconversional rate can be used to determine the isoconversional values of activation energy, E_α, without assuming or determining a particular form of kinetic models [21]. A number of the isoconversional methods have developed and widely used in thermal analyses, mainly including the differential Friedman (Eq. (6)) [22], integral Flynn–Wall–Ozawa (Eq. (7)) [23,24], Kissinger–Akahira–Sunose (Eq. (8)) [25], and Vyazovkin [26–28] methods.

$$\ln\left(\frac{d\alpha}{dt}\right)_\alpha = Const. - \frac{E_\alpha}{RT_\alpha} \tag{6}$$

$$\ln\beta_i = Const. - \frac{1.052E_a}{RT_{\alpha,i}} \tag{7}$$

$$\ln\frac{\beta_i}{T_{\alpha,i}^2} = Const. - \frac{E_\alpha}{RT_{\alpha,i}} \tag{8}$$

In Eqs. (6)–(8), β is the heating rate, and the subscript i indicates a specific temperature program. Among them, the Vyazovkin method, built on the more advanced nonlinear algorithm, has both the high accuracy and the wide applicability to any temperature programs. This method can be generally expressed as Eqs. (9) and (10) for a thermally induced process with linear heating, linear cooling, isothermal, or even more complicated temperature programs.

$$\Phi(E_\alpha) = \sum_{i=1}^{n}\sum_{j\neq i}^{n}\frac{J[E_\alpha, T_i(t_\alpha)]}{J[E_\alpha, T_j(t_\alpha)]} \tag{9}$$

$$J[E_\alpha, T_i(t_\alpha)] \equiv \int_{\alpha-\Delta\alpha}^{t_\alpha}\exp\left[\frac{-E_\alpha}{RT_i(t)}\right]dt \tag{10}$$

In Eqs. (9) and (10), the subscripts, i and j, denote the different thermal experiments, $\Delta\alpha$ is the small conversion increment usually set as 0.02 sufficient to eliminate the systematic error accumulation stemming from the computation process, and the integral J, as recommended by Vyazovkin, can be numerically approached with a trapezoid rule to achieve the sufficient accuracy. Repeat this minimization procedure for each α of interest, and finally an $E_\alpha - \alpha$ relationship will result.

In addition, using these $E_\alpha - T_\alpha$ data, a unified approached has been originally developed to predict isothermal conversion; see Eq. (11) [21,29]:

$$t_\alpha = \frac{\int_0^{t_\alpha}\exp(-E_\alpha/RT_\alpha)dt}{\exp(-E_\alpha/RT_0)} \tag{11}$$

In Eq. (11), t_α is the reaction time for α and T_0 is the isothermal temperature of interest. Specifically, for a nonisothermal process with the constant heating/cooling rate, Eq. (11) can be written as [30]

$$t_\alpha = \frac{\int_0^{T_\alpha}\exp(-E_\alpha/RT_\alpha)dT}{\beta\exp(-E_\alpha/RT_0)} \tag{12}$$

where T_α is the temperature when a nonisothermal reaction processes to a specific conversion, α, with a constant heating rate β at a given isothermal temperature, T_0.

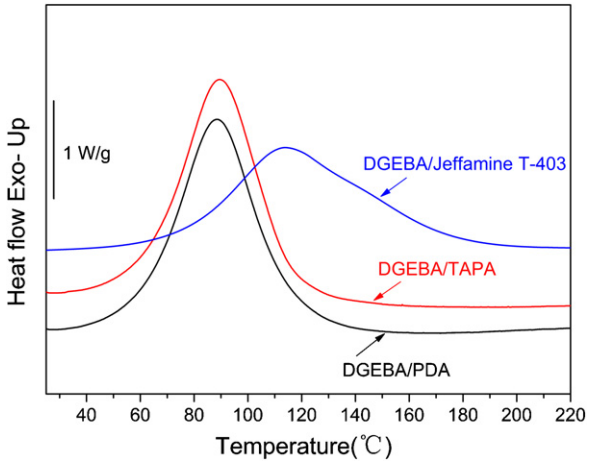

Fig. 1. Nonisothermal DSC thermographs of DGEBA/PDA, DGEBA/TAPA and DGEBA/Jeffamine T-403 with heating rate of 5 °C/min.

4. Results and discussion

4.1. Reactivity of PDA, TAPA and Jeffamine T-403

Fig. 1 shows the dynamic DSC curing curves of DGEBA with PDA, TAPA or Jeffamine T-403 with the heating rate of 5 °C/min, and Table 1 summaries the estimated onset and peak reaction temperatures, T_{onset} and T_{peak}, and reaction heat, ΔH_R. Clearly, DGEBA/PDA and DGEBA/TAPA have very close T_{peak}, T_{onset} and reaction heat with the difference of ≈1 °C and <20 J/g (<5%), indicating that TAPA and PDA exhibit essentially the same reactivity. In contrast, DGEBA/Jeffamine T-403 shows much higher T_{onset} and T_{peak} than the other two reactions, so that Jeffamine T-403 is far less reactive than TAPA and PDA. The higher reactivity of TAPA and PDA is due to the less spatial crowding of the primary amino groups quite different from Jeffamine T-403 (Scheme 1). On the other hand, DGEBA/TAPA, like DGEBA/PDA, liberates the more reaction heat than DGEBA/Jeffamine T-403 (about 21% higher), because TAPA has the much lower amino hydrogen equivalent weight (36.1 g/mol N—H) than Jeffamine T-403 (73.3 g/mol N—H), causing the higher concentration of the epoxy groups in the reaction system.

4.2. Cure of DGEB/TAPA and DGEBA/PDA with multiple heating rate

The DSC thermographs of the nonisothermal curing reactions of DGEBA/PDA and DGEBA/TAPA with the multiple heating rates are presented in Fig. 2. All these curves show a single exothermic peak with good symmetry which is due to the highly exothermic epoxy-amine addition. As the heating rates are increased, the exothermic peaks shift to a higher temperature with the broader peak area. Integrating these exothermic peaks relative to tangent baselines produces such characteristic parameters as the onset and peak cure temperatures, T_{onset} and T_{peak}, and reaction heat, ΔH_R, and Table 2 summarizes their obtained values. These data indicate that increasing the heating rate leads to the systematically increased T_{onset} and T_{peak}, but little affects ΔH_R, implicating that although the heating rates greatly affects the reaction kinetics, they do not change the basic molecular mechanism for the ring-opening involved in the epoxy-amine reaction. By comparison, the two systems show very close T_{onset} and T_{peak} and ΔH_R for each heating rate, which, again, approves that PDA and TAPA have essentially the same reactivity toward epoxy resins.

Table 1
Onset and peak reaction temperatures, T_{onset} and T_{peak}, and reaction heat, ΔH_R, of different systems with heating rate of 5 °C/min.

Formulation	T_{onset} (°C)	T_{peak} (°C)	ΔH_R (J/g)
DGEBA/PDA	60.4	88.5	488.6
DGEBA/TAPA	61.5	89.6	505.7
DGEBA/Jeffamine T-403	76.7	113.8	385.2

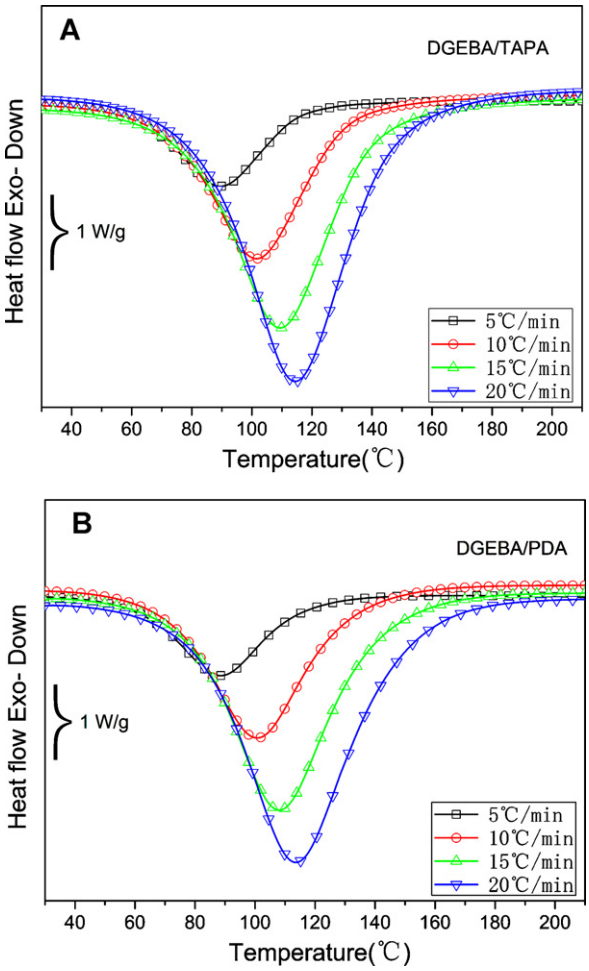

Fig. 2. Nonisothermal DSC thermographs of DGEBA/TAPA (A) and DGEBA/PDA (B) with different heating rates of 5, 10, 15 and 20 °C/min.

Presented in Fig. 3 are the conversional curves of the nonisothermal cure of DGEBA/PDA and DGEBA/TAPA at the different heating rates. These curves exhibit a sigmoidal contour and shift to a higher and broader temperature range with the increased heating rate, demonstrating that the temperature for the reaction to reach the same conversion is systematically increased. This conversion–temperature correlation from the nonisothermal cure of DGEBA/TAPA and DGEBA/PDA will be used for the further model-free isoconversional kinetic analysis, which will be discussed in detail shortly.

4.3. Isothermal cure of DGEB/TAPA and DGEBA/PDA

Illustrated in Fig. 4 are the DSC heat flow-time curves of the isothermal curing reactions of DGEBA/TAPA and DGEBA/PDA at the different temperatures. These DSC traces show only a single exothermic peak without shoulder for each isothermal run, so that the side reactions can be neglected, especially, the etherification reaction among the hydroxyl and amino groups. Nevertheless, the etherification will become significant providing that the reaction temperature is rather high (>150 °C) and the epoxy groups are in

Table 2
Characteristic parameters for nonisothermal cure of DGEBA/TAPA and DGEBA/PDA at heating rates of 5, 10, 15 and 20 °C/min.

Formulation	β (°C/min)	T_{onset} (°C)	T_{peak} (°C)	ΔH_R (J/g)	Mean ΔH_R (J/g)
DGEBA/TAPA	5	60.8	89.5	505.7	515.7
	10	70.9	101.6	522.5	± 7.1
	15	77.7	109.5	516.7	
	20	81.9	114.5	517.7	
DGEBA/PDA	5	60.4	88.5	488.6	504.1
	10	70.3	100.7	515.0	±13.1
	15	76.4	108.1	514.8	
	20	80.1	113.6	497.9	

Table 3
Isothermal reaction exotherm of DGEBA/TAPA and DGEBA/PDA for 40, 50, 60, and 70 °C.

Formulation	Reaction exotherm (kJ/mol epoxide)				
	40 °C	50 °C	60 °C	70 °C	Total
DGEBA/TAPA	80.3 ± 1.6	88.8 ± 1.2	99.7 ± 1.8	103.8 ± 2.0	113.7 ± 2.2
DGEBA/PDA	63.7 ± 1.7	80.7 ± 1.1	95.1 ± 1.6	97.8 ± 2.1	103.0 ± 2.7

excess [31,32]. Integrating the isothermal exothermic peak with respect to the horizontal baseline yields the reaction exotherm, and the sum of the isothermal exotherm and the residual exotherm equals the total reaction heat. From Table 3, as the temperature increases, the isothermal exotherm systematically increases. Noticeably, the total reaction heat still lies in the typical range for the epoxy-amine polymerization (98–122 kJ/mol) [33,34], which evidences that TAPA, similar to conventional linear aliphatic amine curing agents, can crosslink epoxy resins efficiently. Moreover, DGEBA/TAPA exhibits the higher overall molar exotherm than DGEBA/PDA, likely indicating that TAPA reacts with DGEBA more completely than PDA. The reason lies in that TAPA incorporates the more flexible aliphatic chain segments into the reaction system, whereby the chain mobility increased, for which reason the number of the reactive groups topologically isolated in the network is reduced. Such isolated groups are unable to participate the further curing reaction even at higher temperature, in fact, existing as the structural defects in the network, which will negatively affect the properties of the cured epoxy.

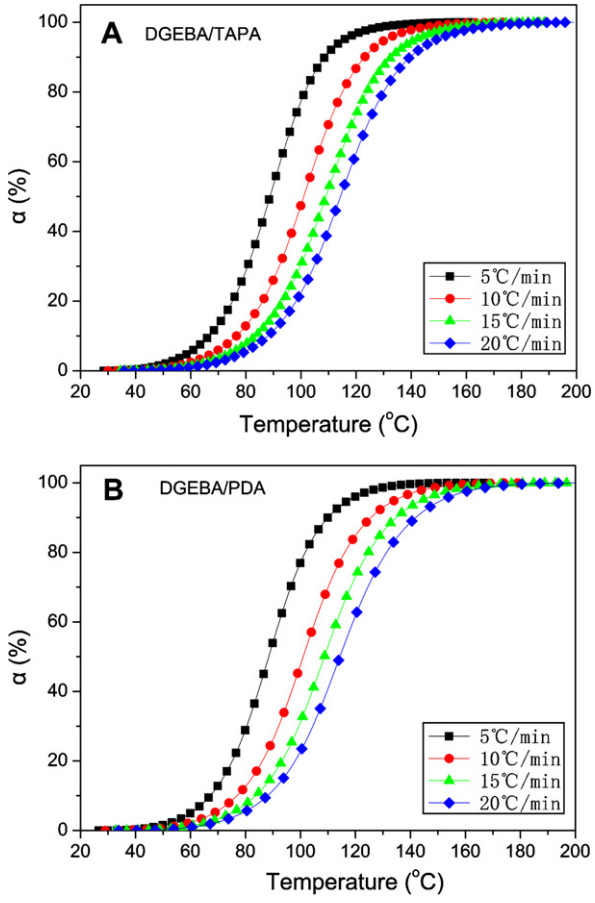

Fig. 3. Conversion curves of nonisothermal reactions of DGEBA/TAPA (A) and DGEBA/PDA (B) with different heating rates of 5, 10, 15 and 20 °C/min.

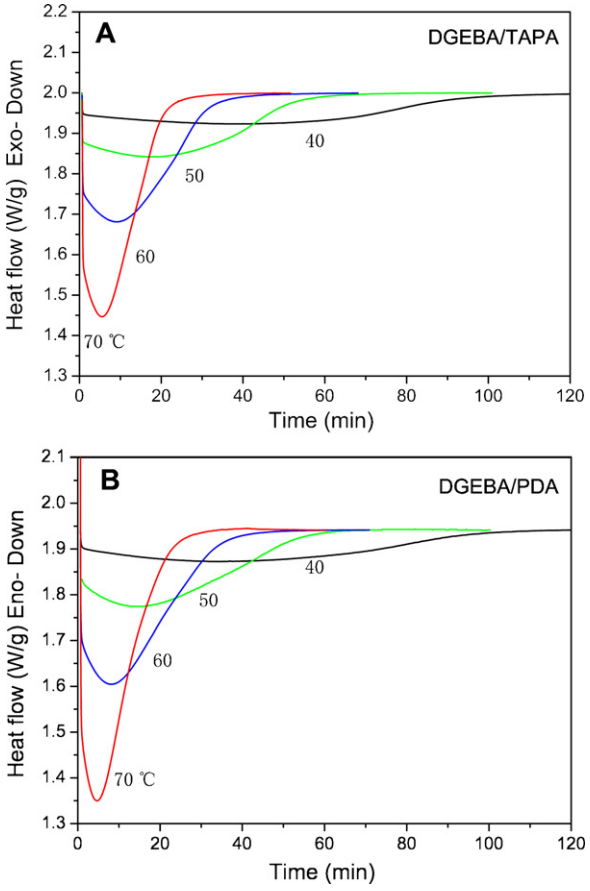

Fig. 4. Isothermal heat flow as a function of curing time at 40, 50, 60 and 70 °C. (A) DGEBA/TAPA and (B) DGEBA/PDA.

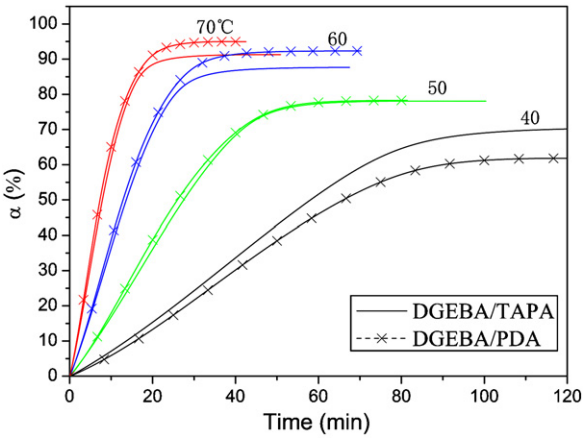

Fig. 5. Conversion–time curves of DGEBA/TAPA (A) and DGEBA/PDA (B) at 40, 50, 60 and 70 °C.

Fig. 5 shows the conversional curves of the isothermal reactions at 40, 50, 60 and 70 °C. α increases rapidly with time initially, and after that the increase becomes slow, eventually the conversional curves leveling off to a limiting conversion, α_T. Increasing the temperature leads to the higher α_T but less than unity, indicating the incompletion of the isothermal cure. Also from Fig. 5, at 40 °C DGEBA/TAPA reacts somewhat faster than DGEBA/PDA with higher α_T achieved, due largely to TAPA introducing the more aliphatic chains in the reaction system, thus decreasing the spatial crowding of the amino functionalities when the reaction is progressing in the higher conversion range. Therefore, the probability of the reaction during the isothermal cure is increased. Moreover, the tertiary amino groups (N^t) of TAPA can likely catalyze the curing reaction [34], resulting in the higher reaction rate. Nevertheless, at the higher temperature (e.g., 70 °C) DGEBA/PDA achieves higher α_T than DGEBA/TAPA, which may be associated with the varied extent of the proximity to the glass temperature of the reaction mixture as the reaction goes. The glass temperatures of the cured epoxy resin will be discussed below.

From the glass-transition curves of the cured epoxy shown in Fig. 6, DGEBA/TAPA has the higher glass temperature, $T_{g\infty}$, than DGEBA/PDA and DGEBA/Jeffamine T-403. Higher $T_{g\infty}$ proves TAPA increases the thermal resistance of the cured epoxy with the higher upper-service temperature, because the glass temperatures are the upper limit for the epoxy materials as the hard plastics.

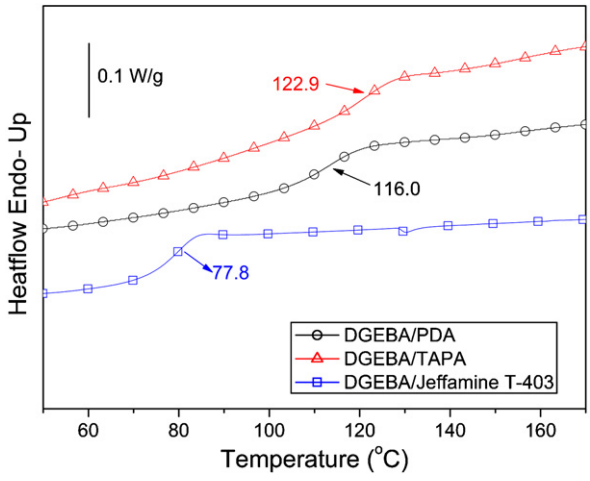

Fig. 6. Glass-transition curves of cured DGEBA/TAPA, DGEBA/PDA and DGEBA/Jeffamine T-403 with heating rate of 10 °C/min.

More strikingly, $T_{g\infty}$ of DGEBA/TAPA is 45 °C higher than that of DGEBA/Jeffamine T-403, indicating significantly improved thermal resistance. Note that TAPA has the higher amine equivalent weight than PDA, 18.5 vs. 37.8 g/mol N—H, thereby introducing the more flexible aliphatic chains in the DGEBA/TAPA network. Despite that, DGEBA/TAPA still exhibits higher $T_{g\infty}$ than DGEBA/PDA, since TAPA provides the cured epoxy network with the extra crosslinks stemming from its branched molecular architecture. Moreover, as discussed above, TAPA can more efficiently cure the epoxy resin as indicated by the higher reaction exotherm, leaving the decreased number of the free dangling chain ends in the network that will increase the free volume. From the analysis above, we can infer that introducing the more flexible aliphatic chains into the epoxy network from the aliphatic amine molecules does not necessarily lead to the decreased glass-transition temperature, and conversely the branched architecture of the aliphatic amine curing agent may moderately increase the thermal resistance of the cured epoxy.

It is worth pointing out that in the addition to the improved thermal resistance TAPA-cured epoxy, TAPA also has the advantages of the low volatility, reduced irritant odor, and extraordinary high functionalities than conventional aliphatic amine curing agents. And, what is more, its raw materials are less expensive and widely available, and the preparation conditions are mild, facilitating its potential mass production and applications. Therefore, TAPA is probably suitable to serve as a radically new aliphatic curing agent with the high reactivity, increased thermal resistance and improved safety combined with the economic benefits, especially for the room-temperature epoxy coatings and adhesives.

4.4. Model-fitting kinetics of isothermal cure

Fig. 7 displays the evolution of the reaction rate, $d\alpha/dt$, with α, from which initially $d\alpha/dt$ increases quickly and goes through the maximum, and increasing the temperature corresponds to the increased peak reaction rate within a shortened time. The maximum $d\alpha/dt$ appearing at the moment, $t > 0$, indicates that the curing reactions follow the autocatalytic mechanism [34–36]. Hence, it is more reasonable to apply the Kamal model (Eq. (3)) to the following model-fitting kinetic analysis. In Eq. (3) k_1 is estimated from the intercept by extrapolating α or t to zero; see Table 4. At 40 °C, DGEBA/TAPA has somewhat higher k_1 than DGEBA/PDA, but at 70 °C the reversed result emerges. Then, the Arrhenius plot of $\ln k_1$ against $1/T$ shown in Fig. 8 can be used to estimate the activation energy for the non-autocatalytic reaction, E_{a1}; see Table 5. The data demonstrate that DGEBA/TAPA has the lower E_{a1} value (61.8 ± 3.1 kJ/mol) than DGEBA/PDA (70.0 ± 4.3 kJ/mol), presumably because the tertiary amino groups (N^t) of TAPA catalyze the epoxy-amine reaction, lowering the energetic barriers for the non-autocatalytic reaction.

Inserting k_1 into Eq. (3), then k_2, m and n, can be estimated using a least-squared procedure (Origin 7.5). As shown in Table 3, k_2 is much greater than k_1, indicating that the autocatalytic reaction is much faster than the non-autocatalytic reaction. Similar to k_1, the Arrhenius plot of k_2 against $1/T$ (Fig. 8) produces the activation energy for the autocatalytic reaction, E_{a2}; see Table 5. These data indicate that for the same reaction system E_{a2} is somewhat lower than E_{a1}, and DGEBA/TAPA (57.2 ± 3.1 kJ/mol) has higher E_{a2} than DGEBA/PDA (47.9 ± 1.6 kJ/mol), causing DGEBA/TAPA shows a far smaller $E_{a1} - E_{a2}$ difference than DGEBA/PDA. The more specific reasons are as follows. First, the —OH groups formed during the cure catalyze the further epoxy-amine reaction, lowering the associated energetic barrier for the autocatalytic reaction [37,38]. Second, the N^t groups of TAPA moderately catalyze the non-autocatalytic reaction, leading to lower intrinsic E_{a1}, and also they may associate with the —OH groups (N···H···O), thereby weakening the catalytic effect of the —OH groups. Nevertheless, the —OH groups catalyze

Table 4
Kinetic parameters of Kamal model for isothermal cure of DGEBA/TAPA and DGEBA/PDA.

Formulation	T_c (°C)	k_1 (min^{-1})	Error	k_2 (min^{-1})	Error	m	Error	n	Error	$m+n$	R^2
DGEBA/TAPA	40	0.00639	3.4×10^{-6}	0.02361	5.0×10^{-5}	0.9287	8.4×10^{-4}	1.14804	1.7×10^{-3}	2.08	0.99528
	50	0.0148	8.3×10^{-6}	0.05233	1.3×10^{-4}	1.01601	1.08×10^{-4}	1.22613	1.64×10^{-3}	2.24	0.99456
	60	0.0296	1.7×10^{-5}	0.09843	2.4×10^{-4}	0.98085	1.19×10^{-3}	1.16916	1.33×10^{-3}	2.15	0.99844
	70	0.0506	4.8×10^{-5}	0.16133	3.7×10^{-4}	0.9345	1.17×10^{-3}	1.14898	1.17×10^{-3}	2.08	0.99923
DGEBA/PDA	40	0.00496	5.3×10^{-6}	0.03213	6.0×10^{-4}	0.89158	6.3×10^{-4}	1.76128	1.79×10^{-3}	2.65	0.99874
	50	0.0136	1.4×10^{-5}	0.0577	1.1×10^{-4}	0.83321	7.9×10^{-4}	1.41007	1.3×10^{-3}	2.24	0.99763
	60	0.0284	4.5×10^{-5}	0.09243	9.0×10^{-5}	0.81872	5.0×10^{-4}	1.12067	5.1×10^{-4}	1.94	0.99974
	70	0.0524	8.5×10^{-5}	0.16449	2.7×10^{-4}	0.83268	8.8×10^{-4}	1.1824	7.8×10^{-4}	2.01	0.99971

Table 5
Activation energies E_a and pre-exponent factor A for autocatalytic and non-autocatalytic reactions of DGEBA/TAPA and DGEBA/PDA.

Formulation	E_{a1} (kJ/mol)	E_{a2} (kJ/mol)	A_1 ($\times10^8$ min^{-1})	A_2 ($\times10^6$ min^{-1})
DGEBA/TAPA	61.8 ± 3.1	57.2 ± 3.1	1.36 ± 0.08	86.5 ± 5.4
DGEBA/PDA	70.0 ± 4.3	47.9 ± 1.6	25.1 ± 1.9	3.18 ± 0.12

the epoxy-amine reaction more effectively than the tertiary amino groups, because they can form the more stable H-bonding with the epoxy ring [34]; otherwise, we should not observe the apparent autocatalytic phenomenon for DGEBA/TAPA. In addition to the activation energies, the estimated reaction orders, m and n, vary moderately as the temperature rises, reflecting the complex nature of the reaction mechanisms [39].

Introducing the value of k_1, k_2, m and n in Eq. (3) yields the rate equations. The experimental rates and the predicated from these rate equations are compared in Fig. 9, where the full lines are the experimental rates, while the separated dots are the predicated. Clearly, the experimental rates accord well with the predicted at the early stage, but at the high conversion, the obvious discrepancy appears because of the diffusion-controlled reaction kinetics. Moreover, increasing the isothermal temperature delays this deviation to a higher conversion, because of the enhanced chain mobility in the network at the higher temperature. Therefore, the Kamal model is able to satisfactorily describe the reaction-controlled kinetic rate, yet is still insufficient in depicting the diffusion-controlled reaction kinetics.

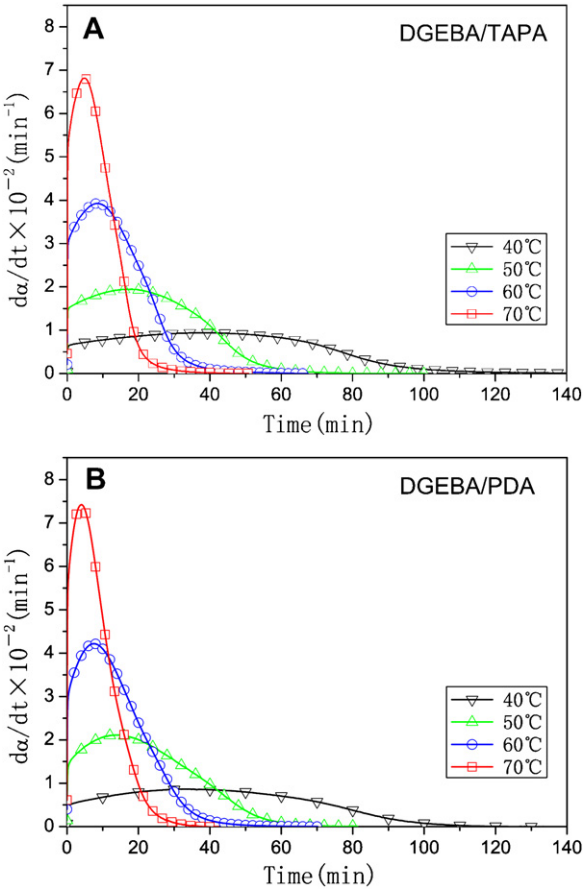

Fig. 7. Variation of $d\alpha/dt$ with time t of DGEBA/TAPA (A) and DGEBA/PDA (B).

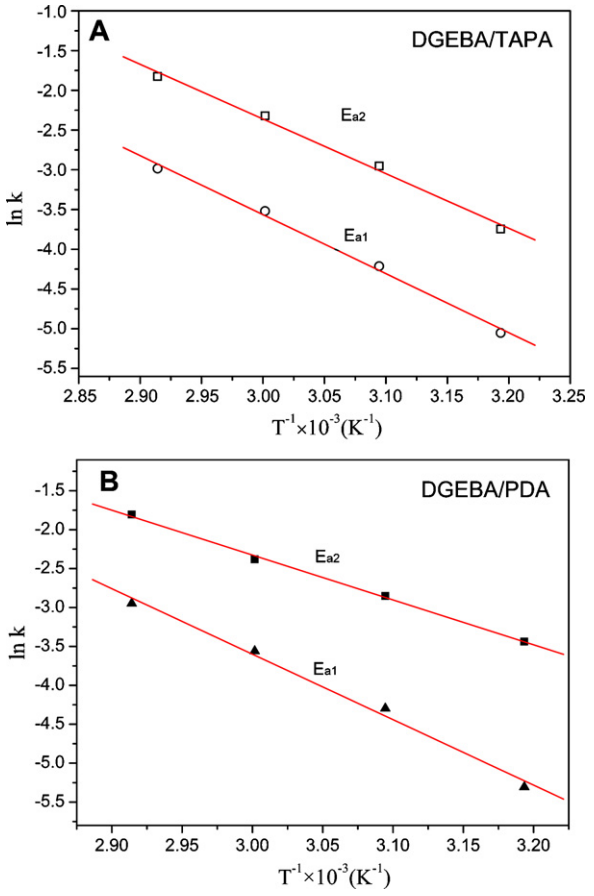

Fig. 8. Arrhenius plots of $\ln k_1$ and $\ln k_2$ vs.$1/T$. for DGEBA/TAPA (A) and DGEBA/PDA (B).

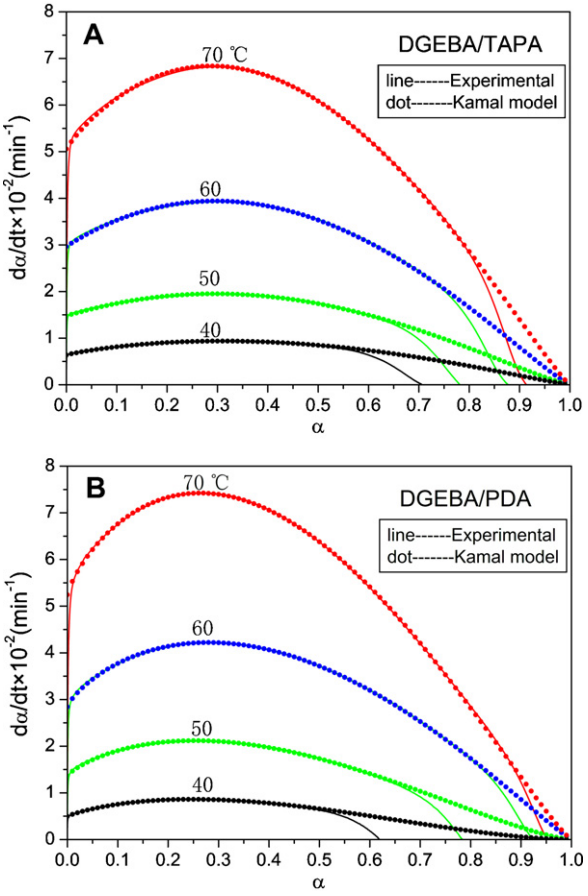

Fig. 9. Comparison of experimental $d\alpha/dt$ and predicated from Kamal model. (A) DGEBA/TAPA and (B) DGEBA/PDA.

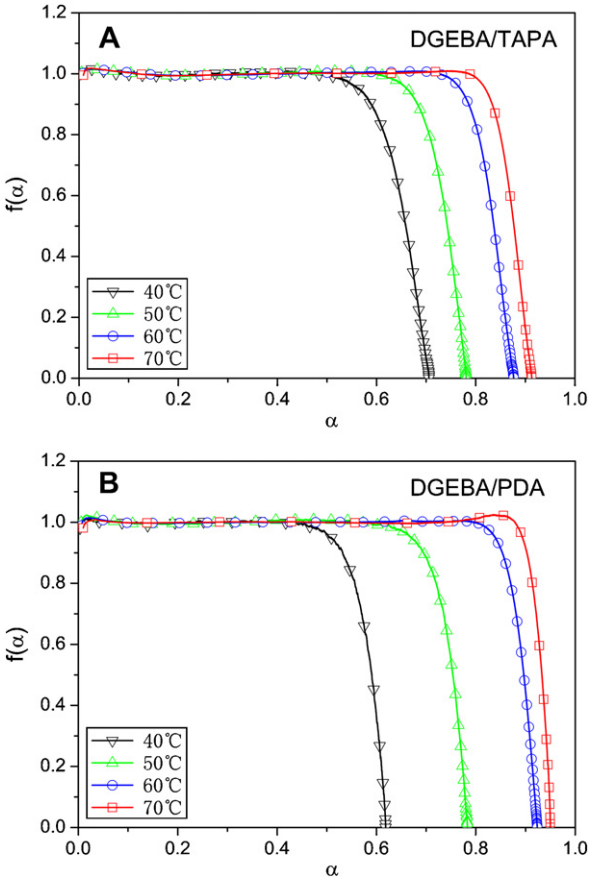

Fig. 10. Diffusion factor $f(\alpha)$ vs. α for DGEBA/TAPA (A) and DGEBA/PDA (B) at 40, 50, 60 and 70 °C.

Cole [40] proposed a modified version of the Kamal model concerning diffusion control; see Eq. (13):

$$\frac{d\alpha}{dt} = [k_1(T) + k_2(T)\alpha^m](1-\alpha)^n f(\alpha) \tag{13}$$

where diffusion factor $f(\alpha)$ is the ratio of the effective rate constant to pure chemical reaction rate constant.

$$f(\alpha) = \frac{k_e}{k_c} = \frac{1}{1+\exp[C(\alpha-\alpha_c)]} \tag{14}$$

In Eq. (14), k_e is the effective rate constant, k_c is the chemical reaction rate constant, C is the fitting constant, and α_c is the critical conversion indicating the change of chemical reaction to diffusion control.

$f(\alpha)$ as a function of conversion α for DGEBA/TAPA and DGEBA/PDA is demonstrated in Fig. 10, from which $f(\alpha)$ approximately equals unity at the low conversion stage, but in the deep-conversion stage, drops quickly, approaching zero, in which case the reaction becomes very slow and practically stops [41]. Moreover, increasing the temperature delays the decrease of $f(\alpha)$ to a higher conversion range, due to the enhanced the mobility of the reactive species. In summary, the curing reactions first experience the reaction-controlled region, then the diffusion control comes at the higher temperature range, and the diffusion-controlled kinetics is extremely sensitive to the reaction temperature.

Eq. (14) is used to fit the experimental data presented in Fig. 10 with a least-squared procedure (Origin 7.5), and the calculated values of the unknowns, C and α_c, are compared in Table 6. In general, α and C increase gradually with the increased temperature, reflecting the delay of the diffusion control to the higher conversion range. In addition, the reaction temperatures seem to influence α_c of DGEBA/PDA more than that of DGEBA/TAPA, if the temperature is relatively low (40–50 °C). The reason may be that TAPA introduces the more flexible aliphatic chains in the network than PDA, leading to the enhanced mobility of the reactive amino and epoxy groups to diffuse into the tangible distance to trigger the curing reaction even at the relatively low reaction temperature.

So far, a complete set of the kinetic parameters have been identified for the extended Kamal model. Introducing their values into Eq. (13) yields the ultimate rate equations to predict the isothermal cure. In Fig. 11, the experimental reaction rate (lines) and the model predicted (dotes) are compared, with an excellent match achieved; therefore, the extended Kamal model is able to adequately depict the isothermal curing reaction rate over the entire conversion range.

4.5. Model-free isoconversional kinetic analysis

So far, we have accomplished the model-fitting kinetic analysis of DGEBA/PDA and DGEBA/TAPA, and subsequently we will use the Vyazovkin method [27,28] to conduct the model-free isoconversional kinetic analysis. With this method, Eq. (10), we obtain the effective activation energy, E_α, as a function of α for the isothermal and nonisothermal curing reactions of DGEBA/TAPA and DGEBA/PDA. As shown in Fig. 12, E_α changes substantially with α, especially for the isothermal reactions, which implicates that the reactions may involve the multi-step kinetic pathways with the varying energetic barriers [42–44]. The detailed analysis of this correlation is as follows.

Table 6
Values of critical conversion, α_c, and fitting constant, C, of isothermal DGEBA/TAPA and DGEBA/PDA reactions.

Formulation	T_c	40 °C	50 °C	60 °C	70 °C
DGEBA/TAPA	α_c	0.65515 ± 0.00006	0.73969 ± 0.00008	0.83488 ± 0.00007	0.87579 ± 0.00008
	C	47.3 ± 0.10	68.67 ± 0.25	69.28 ± 0.23	79.91 ± 0.32
	R^2	0.99398	0.98997	0.99388	0.99349
DGEBA/PDA	α_c	0.58626 ± 0.0001	0.75005 ± 0.00007	0.89441 ± 0.00006	0.93113 ± 0.00007
	C	72.92 ± 0.39	73.42 ± 0.30	92.25 ± 0.38	128.39 ± 0.84
	R^2	0.98513	0.98718	0.99009	0.98442

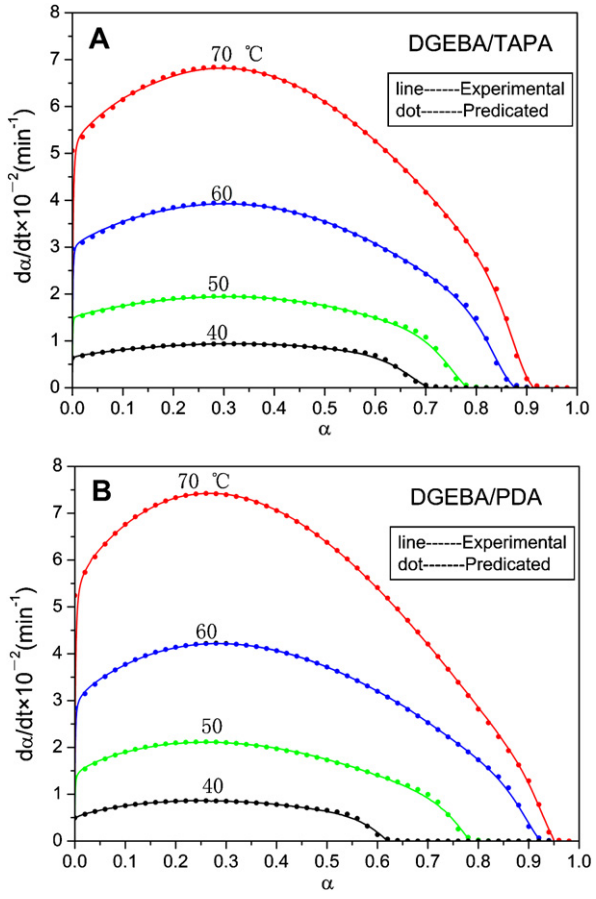

Fig. 11. Comparison of experimental reaction rates of DGEBA/TAPA and DGEBA/PDA and those predicated from extended Kamal model for 40, 50, 60 and 70 °C.

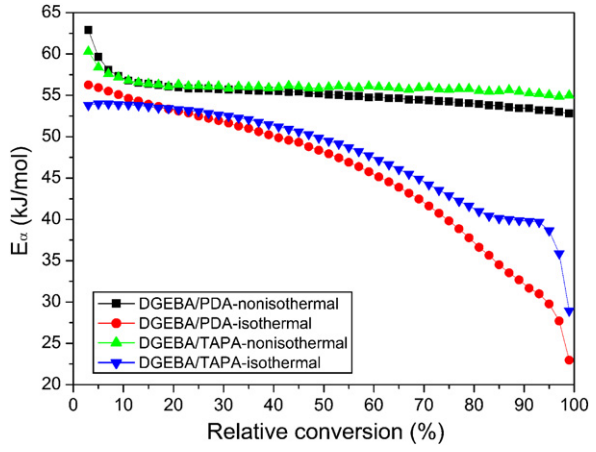

Fig. 12. Effective activation energy E_α as a function relative conversion for isothermal and nonisothermal curing reactions of DGEBA/TAPA and DGEBA/PDA.

For the isothermal cure, DGEBA/TAPA exhibits somewhat the lower initial E_α value than DGEBA/PDA, which resembles the case of E_{a1} discussed in the previous section (Table 4). This resemblance demonstrates again that the tertiary groups of TAPA additionally catalyze the epoxy-amine reaction compared to PDA. As α increases, DGEBA/TAPA shows relatively constant E_α up to $\alpha \approx 0.3$, whereas E_α of DGEBA/PDA decreases gradually. This likely reflects that the —OH groups formed during the cure affect DGEBA/PDA more than DGEBA/TAPA, because the tertiary amine groups of TAPA catalyze the DGEBA/TAPA reaction, leading to the lowered energetic barrier for the non-autocatalytic reaction, and they could also associated with the —OH groups, decreasing the —OH catalytic ability. Once α exceeds 0.3, E_α of DGEBA/TAPA begins to decrease and later arrives at the plateau (Fig. 10), whereas the steady decrease in E_α occurs for DGEBA/PDA. This difference likely indicates that DGEBA/PDA is affected more by the diffusion than DGEBA/TAPA, which is like attributed to TAPA introducing the more aliphatic chains in the reaction system, causing the less restricted diffusion of the reactive groups.

While the isothermal curing reactions are progressing in the deep-conversion stage, the steep decrease in E_α appears, which indicates that the system begins to vitrify and the diffusion controls the reaction rate [42]. In this case, the diffusion of the reactive species is greatly inhibited, and thus the further reaction can only relay on the short-range motions of the adjacent reactive species. Note here that $T_{g\infty}$ (>110 °C) of the cured epoxy (see Fig. 6) is much higher that the isothermal temperatures (≤70 °C), thus the vitrification will certainly occur during the isothermal cure. The vitrification-induced diffusion-controlled kinetics is also supported by a previous finding that while the curing reaction of thermosets carrying out at the glass-transition stages, it exhibited the very low activation energies [45,46]. Finally, DGEBA/TAPA shows somewhat higher E_α than DGEBA/PDA, because the more flexible aliphatic molecular chains from TAPA make the segmental motions caused by the configuration adjustments in the DGEBA/TAPA network less restricted, compared to the DGEBA/PDA network with the higher more rigid bisphenol A content.

In contrast, E_α of the nonisothermal reaction behaviors quite unlike the corresponding isothermal cure discussed above. To illustrate, at the initial cure stage, E_α of the two system decreases quickly with α, due primarily to the marked decrease in the viscosity of the reaction mixture, thereby the energetic barrier for the diffusion of the molecules lowered. More interestingly, DGEBA/PDA shows the somewhat higher initial E_α value than DGEBA/TAPA, which accords with the case of the corresponding isothermal cure. Clearly, the reason for this finding is that the tertiary amine of TAPA catalyzes the reaction, irrespective of the isothermal or nonisothermal temperature programs used to cure the epoxy-amine mixture. Moreover, in generally, the nonisothermal cure exhibits higher E_α than the corresponding isothermal cure, and after the initial cure stage ($\alpha > 0.15$) shows a relatively constant E_α value of 53–57 kJ/mol, in contrast to the dramatic decrease in E_α observed from the isothermal cure in the deep conversion stage. Relatively stable E_α likely indicates that the nonisothermal reaction has reached a dynamic balance, at which state the conversion, temperature, viscosity, crosslink

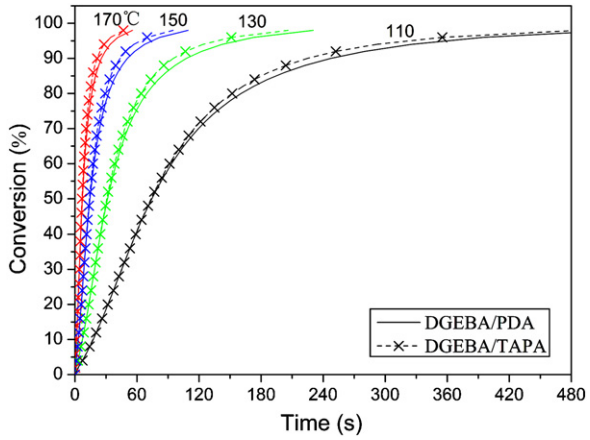

Fig. 13. Isothermal conversion at 110, 130, 150 and 170 °C predicted from non-isothermal data using Eq. (12).

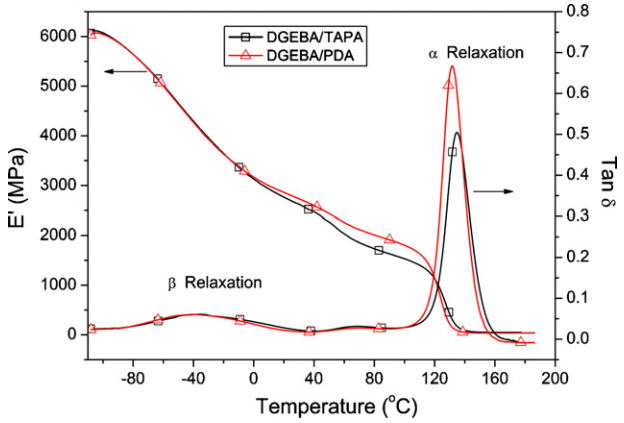

Fig. 14. Dynamic mechanical spectra for E' and $\tan\delta$ at heating rate of 3 °C/min (1 Hz).

density, chain mobility, etc. may achieve a certain compromise. This observation is quite different from the isothermal cure. To illustrate, because the temperature keeps constant for the isothermal cure, thus the motion of polymeric chains bearing the reactive groups will become more and more restricted as the conversion and the number of the crosslinks increase. For this reason, the diffusion will play an increasingly important role in determining the isothermal curing kinetics, eventually the macroscopic reaction traversing the reaction-controlled stage gradually deep into diffusion-controlled regime, with the quick drop in E_α observed. Therefore, we can infer that the nonisothermal cure is little affected by the diffusion-controlled kinetics without the dramatic decrease in E_α detected in the high conversion stage.

4.6. Model-free prediction of isothermal conversion at higher temperatures

It is of practical interest to predict the epoxy curing reaction outside the experimental temperature range, which will be helpful in selecting the appropriate curing cycles according to specific applications. From the analysis above, we have used the extended Kamal model to successfully describe the isothermal temperatures of 40, 50, 60, and 70 °C. But it is still hard for us to collect the reliable isothermal curing kinetic data at even the higher experimental temperature range for the experiment and instrument reasons. For example, the much higher isothermal temperature results in the very fast reaction rate, in which case the stabilization time to the appointed isothermal temperature will become so long that the unregistered reaction heat is too large to be acceptable, thus causing the unreliable kinetic data. To predict the isothermal curing rate at the isothermal temperature much higher than our isothermal experiment temperatures (e.g., >100 °C), the model-free isoconversional method may be a good alternative. Notice that because the diffusion-controlled kinetics can be neglected for the nonisothermal cure, thus it is more reasonable to use the model-free method from the nonisothermal data to predict the isothermal cure at the higher temperatures, in which case the diffusion control is insignificant.

Fig. 13 illustrates the predicted isothermal curing rate of DGEBA/TAPA and DGEBA/PDA at 110, 130, 150 and 170 °C. At the beginning, the conversion increases steeply, and at the late stage the increase becomes slower and slower up to the completion of the isothermal cure. In this temperature range, the entire reaction will only spend from about half a minute to a few minutes. Moreover, DGEBA/TAPA and DGEBA/PDA behaviors quite like at the early stage of the cure, and at the higher conversion stage, the conversion of the former is slightly higher than that of the latter, the reason for which is that the more aliphatic chains present in the DGEBA/TAPA system, leading to the easier diffusion of the reactive species. The very fast curing speed will result in the very acute heat release, which should be avoided in practical applications; otherwise, the reaction will be out of control unless removing the accumulated reaction exotherm in time. Thus, to facilitate the dissipation of the reaction heat it is more reasonable to use TAPA to cure epoxy resins at the relatively low temperatures (e.g., room temperature) for a relatively long time (several hours) to finish the most percentage of the cure, and after that, if necessary, the post-cure at higher temperatures (e.g., >100 °C) for a short time can be applied to yield the more completely crosslinked network to result in the improved thermal resistance, especially the glass temperature.

4.7. Dynamic mechanical properties of cured epoxy

Fig. 14 displays the dynamic mechanical spectra for storage modulus E' and loss factor $\tan\delta$ of the DGEBA/TAPA and DGEBA/PDA networks with the heating rate of 3 °C/min (1 Hz), where E' and $\tan\delta$ are plotted against the temperature. At the lower temperature range (−100 to −20 °C), the two networks have very close E' (Table 7), but once the temperature exceeds −20 °C, DGEBA/TAPA loses E' more than DGEBA/PDA. Moreover, a sub-glass relaxation (β relaxation) can be found from the $\tan\delta$ profiles, stemming from the hydrogen-bonded $-CH_2CH(OH)CH_2-$ sequences [47–50]. DGEBA/TAPA (−35.2 °C) exhibits the higher β-transition temperature than DGEBA/PDA (−39.9 °C), implying that the even localized $-CH_2CH(OH)CH_2-$ motions in the former network are more restricted than those in the latter. Nevertheless, the β-relaxation temperatures of the two networks differ still small, indicating that the origination of the β relaxation is not changed.

Table 7
Relaxation temperatures, characteristic modulus and crosslink density of DGEBA/TAPA and DGEBA/PDA networks.

Formulation	DGEBA/TAPA	DGEBA/PDA
α-Relaxation (T_g)/°C	134.9	131.8
Peak height ($\tan\delta_\alpha$)	0.505	0.667
β-Relaxation (T_β)/°C	−35.2	−39.9
Peak height ($\tan\delta_\beta$)	0.0607	0.0605
Modulus at −100 °C/MPa	6074	6044
Modulus at 20 °C/MPa	2763	2860
Modulus at 80 °C/MPa	1734	2011
Rubber modulus/MPa	50	37
Crosslink density/(mol/m^3)	4576	3144

As the temperature further rises, E' of DGEBA/PDA exceeds that of DGEBA/TAPA at an ambient temperature range (>0 °C); see Fig. 14 and Table 7. This finding is likely contrary to the common intuition that the increased crosslink density corresponds to the more rigid network, exhibiting higher E', but really resembles the previous finding that the higher the crosslink density of epoxy-amine networks, the lower elastic modulus they exhibit [51]. In fact, DGEBA/TAPA has the higher crosslink density than DGEBA/PDA, which will be analyzed in detail soon. Lower E' is largely associated with the damping during the β relaxation; for example, the higher crosslink density and the more aliphatic segments of the DGEBA/TAPA network will increase the dissipation of the elastic energy as a result of the more the out-phase plastic deformation of chains.

At the higher temperature, E' decreases abruptly from >1000 MPa to <100 MPa (Table 7) in a narrow temperature range; meanwhile, tan δ reaches its maximum with the peak height much higher than that of the β relaxation. This observation means that the two networks undergo the glass-rubber transition (α relaxation), and after that the glassy epoxy network transforms into a high elastic rubber. Herein the rubbery modulus, E_r, shown in Table 7 is taken as the storage modulus at 30 °C above the glass temperature [52]. DGEBA/TAPA has higher E_r than DGEBA/PDA, which probably indicates that the former has the increased crosslink density and reduced average molecular weight between the two adjacent crosslinks. To be quantitative, we estimate the crosslink density from Eq. (15) [53]:

$$E_r = 3RT_r\nu_e \quad (15)$$

where R is the universal gas constant, T_r is the temperature corresponding to E_r, and ν_e is the crosslink density. As shown in Table 7, DGEBA/TAPA has much higher ν_e than DGEBA/PDA. Increased ν_e is due to the fact that TAPA has the two tertiary amine groups (N^t) (see Scheme 1) functioning as the additional crosslinks in the cured epoxy network. Note here that although TAPA has the much higher N—H equivalent weight (37.8 g/mol N—H) than propanediamine (18.5 g/mol N—H), facilitating weighting and mixing, its branched molecular architecture contributes more to the crosslink density. As a result, DGEBA/TAPA has the higher crosslink density than DGEBA/PDA with the higher glass temperature.

A further analysis of Fig. 14 and Table 7 indicates that during the glass transition stage, E' of DGEBA/TAPA changes less dramatically compared to DGEBA/PDA, and the peak height is lower, too. The reason is as follows. The increased crosslink density corresponds to the shortened average chain length among the crosslinks, so that the viscous plastic deformation of the network becomes more difficult, reducing the elastic energy dissipation during the cooperative motions of the whole DGEBA/TAPA network chains under the stress.

4.8. Thermal stability

Fig. 15 displays the TG thermographs of cured DGEBA/TAPA and DGEBA/PDA. Clearly, they remain thermally stable up to ~300 °C, and DGEBA/PDA starts to decompose at a slightly higher temperature. The high decomposition temperature suggests TAPA, comparable to aliphatic amine curing agents like PDA, can endow the epoxy resin with the sufficient thermal stability. The high thermal stability is due to the TAPA molecules consisting solely of the nitrogen–carbon (N—C), carbon–carbon (C—C), nitrogen–hydrogen (N—H) and carbon–hydrogen (C—H) single bonds identical with the common aliphatic amines. Such kinds of the chemical bonds have the considerably high cleavage energies, enabling the thermal scission of TAPA moieties in the epoxy network at the high temperature. In contrast to these more stable bonds, the thermal rapture of cured epoxy-amine products generally starts from the

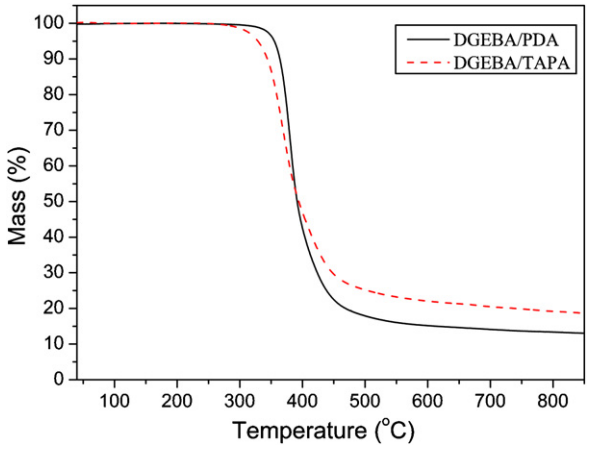

Fig. 15. TG thermographs of cured DGEBA/TAPA and DGEBA/PDA with 10 °C/min in N_2.

emission of the water from the secondary alcohol groups, leading to the formation of the vinylene ethers [54], which can account for why the DGEBA/TAPA and DGEBA/PDA have the close initial thermal decomposition temperatures.

Once the temperature rises above 300 °C, the epoxy resin starts to decompose rapidly and the most mass loses within 300–500 °C. In this stage, the chain scission of the networks yields the combustible gases, water, amines, and gaseous aromatic compounds, etc. [54]. Note here that DGEBA/TAPA has the higher char yield at 800 °C than DGEBA/PDA, which substantiates that TAPA endows the cured epoxy with the improved flame retardance, due likely to the higher crosslink density but the lower oxygen content of the TAPA-cured epoxy, compared to DGEBA/PDA. Especially, the higher crosslink network may promote the charring of the cured epoxy resin during the pyrolysis, since the increased number of the chemical bonds presents in the cured epoxy. To summarize, similar to common aliphatic amines like PDA, TAPA endows the cured epoxy with the adequate thermal stability to satisfy rational-service-temperature applications.

5. Conclusions

We have systematically investigated and compared the three aliphatic amine epoxy curing agents: TAPA, PDA and Jeffamine T-403. The dynamic DSC evidenced that TAPA and PDA had the very close reactivity much higher than that of Jeffamine T-403, and TAPA could more sufficiently cure DGEBA than PDA with the higher molar reaction exotherm. TAPA imparted the cured epoxy with the higher glass temperature than PDA which is 45 °C higher than that of Jeffamine T-403-cured epoxy. The isothermal DSC indicated that TAPA could increase the conversion at the lower temperature (e.g., 40 °C). The isothermal cure was proved autocatalytic, and the Kamal model was able to well describe the kinetic rate within the reaction-controlled zone. DGEBA/TAPA had the higher non-autocatalytic reaction activation energy (61.8 ± 3.1 kJ/mol) than DGEBA/PDA (70.0 ± 4.3 kJ/mol) owing to the catalytic tertiary amine groups of TAPA. The further investigation showed that the extended Kamal model considering the diffusion effect could sufficiently predict the entire isothermal cure.

The model-free kinetic analysis demonstrated the effective activation energy, E_α, changed with the conversion markedly, reflecting change of the reaction kinetic schemes. In particular, the isothermal reaction shifted from the reaction to diffusion control in the higher conversion, but the diffusion control little affected the nonisothermal reaction. In comparison, DGEBA/TAPA had lower initial E_α than DGEBA/PDA, analogue to the non-autocatalytic reaction activation

energy. In the deep cure stage, DGEBA/TAPA showed higher E_α, due to the more flexible aliphatic chains of TAPA that increase the chain mobility of the network. Furthermore, the isothermal conversion at the temperatures much higher than the isothermal experiment temperature was reasonably predicted from the non-isothermal experiments using the model-free Vyazovkin method. The result illustrated that it is more reasonable for TAPA to cure the epoxy resin according to a two-step schedule: the cure at the lower temperatures (e.g., room temperature) for a relatively long time to relieve the reaction heat, followed by the post cure at higher temperature (e.g., 100 °C) for a short time to further improve the glass temperature.

DMA confirmed DGEBA/TAPA had the higher glass- and β-relaxation temperatures, and, more important, TAPA endowed the cured epoxy with the higher crosslink density attributable to branched molecular architecture. The TG analysis disclosed DGEBA/TAPA had sufficient thermal stability, with the initial decomposition temperature up to 300 °C, and compare to PDA, TAPA could increase the char yield at the high temperature.

In summary, TAPA has the high reactivity to well cure epoxy resins, extraordinarily high functionalities, and extended stoichiometry combined with favorable features of the low volatility, inexpensive raw materials, and facile preparation conditions. Also, TAPA imparts the cured epoxy with the high crosslink density, glass temperature, and thermal stability. Owing to these outstanding properties, TAPA shows the high promising as a radically new aliphatic amine curing agents for epoxy resins, especially for the fast-cure, quick-dry room-temperature epoxy coatings and adhesives.

Acknowledgments

This work was supported by the Program for Changjiang Scholars and Innovative Research Team in University, China (PCSIRT) and the Major Research Project of Zhejiang Province (Grant No. 2006C11192). Special thanks are due to the reviewers for providing the very helpful comments.

Appendix A. Supplementary data

Supplementary data associated with this article can be found, in the online version, at doi:10.1016/j.cej.2012.01.134.

References

[1] N.A.S. John, G.A. George, Diglycidyl amine-epoxy resin networks: kinetics and mechanisms of cure, Prog. Polym. Sci. 19 (1994) 755–795.
[2] B.K. Kandola, B. Biswas, D. Price, A.R. Horrocks, Studies on the effect of different levels of toughener and flame retardants on thermal stability of epoxy resin, Polym. Degrad. Stab. 95 (2010) 144–152.
[3] D. Zhang, D. Jia, S. Chen, Kinetics of curing and thermal degradation of hyperbranched epoxy (HTDE)/diglycidyl ether of bisphenol-A epoxy hybrid resin, J. Therm. Anal. Calorim. 98 (2009) 819–824.
[4] R. Mezzenga, L. Boogh, J.A.E. Manson, B. Pettersson, Effects of the branching architecture on the reactivity of epoxy-amine groups, Macromolecules 33 (2000) 4373–4379.
[5] D. Zhang, D. Jia, S. Chen, Synthesis and characterization of low viscosity aromatic hyperbranched poly(trimellitic anhydride ethylene glycol) ester epoxy resin, Macromol. Chem. Phys. 210 (2009) 1159–1166.
[6] D. Zhang, D. Jia, Synthesis of novel low-viscosity liquid epoxidized aromatic hyperbranched polymers, Eur. Polym. J. 42 (2006) 711–714.
[7] J. Wan, B.-G. Li, H. Fan, Z.-Y. Bu, C.-J. Xu, Nonisothermal reaction, thermal stability and dynamic mechanical properties of epoxy system with novel nonlinear multifunctional polyamine hardener, Thermochim. Acta 511 (2010) 51–58.
[8] A. Nohales, L. Solar, I. Porcar, C.I. Vallo, C.M. Gómez, Morphology, flexural, and thermal properties of sepiolite modified epoxy resins with different curing agents, Eur. Polym. J. 42 (2006) 3093–3101.
[9] H. Cai, P. Li, G. Sui, Y. Yu, G. Li, X. Yang, S. Ryu, Curing kinetics study of epoxy resin/flexible amine toughness systems by dynamic and isothermal DSC, Thermochim. Acta 473 (2008) 101–105.
[10] R.J. Morgan, F.-M. Kong, C.M. Walkup, Structure-property relations of polyethertriamine-cured bisphenol-A-diglycidyl ether epoxies, Polymer 25 (1984) 375–386.
[11] Y. Calventus, S. Montserrat, J.M. Hutchinson, Enthalpy relaxation of non-stoichiometric epoxy-amine resins, Polymer 42 (2001) 7081–7093.
[12] J. Wan, Z.-Y. Bu, C.-J. Xu, H. Fan, B.-G. Li, Model-fitting and model-free non-isothermal curing kinetics of epoxy resin with a low-volatile five-armed starlike aliphatic polyamine, Thermochim. Acta 525 (2011) 31–39.
[13] J. Wan, Z.-Y. Bu, C.-J. Xu, B.-G. Li, H. Fan, Preparation, curing kinetics, and properties of a novel low-volatile starlike aliphatic-polyamine curing agent for epoxy resins, Chem. Eng. J. 171 (2011) 357–367.
[14] J. Wan, Z.-Y. Bu, C.-J. Xu, B.-G. Li, H. Fan, Learning about novel amine-adduct curing agents for epoxy resins: butyl-glycidylether-modified poly(propyleneimine) dendrimers, Thermochim. Acta 519 (2011) 72–82.
[15] J. Wan, B.-G. Li, H. Fan, Z.-Y. Bu, C.-J. Xu, Nonisothermal reaction kinetics of DGEBA with four-armed starlike polyamine with benzene core (MXBDP) as novel curing agent, Thermochim. Acta 510 (2010) 46–52.
[16] C. Wörner, R. Mülhaupt, Polynitrile- and polyamine-functional poly(trimethylene imine) dendrimers, Angew. Chem. Int. Ed. Engl. 32 (1993) 1306–1308.
[17] M.M.d.B.-v.d.B. Ellen, E.W. Meijer, Poly(propylene imine) dendrimers: large-scale synthesis by hetereogeneously catalyzed hydrogenations, Angew. Chem. Int. Ed. Engl. 32 (1993) 1308–1311.
[18] H.J. Borchardt, F. Daniels, The application of differential thermal analysis to the study of reaction kinetics, J. Am. Chem. Soc. 79 (1957) 41–46.
[19] S. Sourour, M.R. Kamal, Differential scanning calorimetry of epoxy cure: isothermal cure kinetics, Thermochim. Acta 14 (1976) 41–59.
[20] R.K. Musa, Thermoset characterization for moldability analysis, Polym. Eng. Sci. 14 (1974) 231–239.
[21] S. Vyazovkin, A.K. Burnham, J.M. Criado, L.A. Pérez-Maqueda, C. Popescu, N. Sbirrazzuoli, ICTAC kinetics committee recommendations for performing kinetic computations on thermal analysis data, Thermochim. Acta 520 (2011) 1–19.
[22] H.L. Friedman, Kinetics of thermal degradation of char-forming plastics from thermogravimetry. Application to a phenolic plastic, J. Polym. Sci. C 6 (1964) 183–195.
[23] J.H. Flynn, L.A. Wall, General treatment of the thermogravimetry of polymers, J. Res. Natl. Bur. Stand. A Phys. Chem. 70A (1966) 487–523.
[24] T. Ozawa, A new method of analyzing thermogravimetric data, Bull. Chem. Soc. Jpn. 38 (1965) 1881–1886.
[25] T. Akahira, T. Sunose, Method of determining activation deterioration constant of electrical insulating materials, Res. Report Chiba Inst. Technol. (Sci. Technol.) 16 (1971) 22–31.
[26] S. Vyazovkin, D. Dollimore, Linear and nonlinear procedures in isoconversional computations of the activation energy of nonisothermal reactions in solids, J. Chem. Inf. Comput. Sci. 36 (1996) 42–45.
[27] S. Vyazovkin, Evaluation of activation energy of thermally stimulated solid-state reactions under arbitrary variation of temperature, J. Comput. Chem. 18 (1997) 393–402.
[28] S. Vyazovkin, Modification of the integral isoconversional method to account for variation in the activation energy, J. Comput. Chem. 22 (2001) 178–183.
[29] S. Vyazovkin, Model-free kinetics staying free of multiplying entities without necessity, J. Therm. Anal. Calorim. 83 (2006) 45–51.
[30] S. Vyazovkin, A unified approach to kinetic processing of nonisothermal data, Int. J. Chem. Kinet. 28 (1996) 95–101.
[31] C.C. Riccardi, R.J.J. Williams, Statistical structural model for the build-up of epoxy-amine networks with simultaneous etherification, Polymer 27 (1986) 913–920.
[32] C.C. Riccardi, R.J.J. Williams, A kinetic scheme for an amine-epoxy reaction with simultaneous etherification, J. Appl. Polym. Sci. 32 (1986) 3445–3456.
[33] Y. Zhang, S. Vyazovkin, Comparative cure behavior of DGEBA and DGEBP with 4-nitro-1,2-phenylenediamine, Polymer 47 (2006) 6659–6663.
[34] B.A. Rozenberg, Kinetics, thermodynamics and mechanism of reactions of epoxy oligomers with amines, Adv. Polym. Sci. 75 (1986) 113–165.
[35] M.R. Keenan, Autocatalytic cure kinetics from DSC measurements: zero initial cure rate, J. Appl. Polym. Sci. 33 (1987) 1725–1734.
[36] Z. Ma, J. Gao, Curing kinetics of o-cresol formaldehyde epoxy resin and succinic anhydride system catalyzed by tertiary amine, J. Phys. Chem. B 110 (2006) 12380–12383.
[37] I.T. Smith, The mechanism of the crosslinking of epoxide resins by amines, Polymer 2 (1961) 95–108.
[38] J.E. Ehlers, N.G. Rondan, L.K. Huynh, H. Pham, M. Marks, T.N. Truong, Theoretical study on mechanisms of the epoxy-amine curing reaction, Macromolecules 40 (2007) 4370–4377.
[39] N. Sbirrazzuoli, A. Mititelu-Mija, L. Vincent, C. Alzina, Isoconversional kinetic analysis of stoichiometric and off-stoichiometric epoxy-amine cures, Thermochim. Acta 447 (2006) 167–177.
[40] K.C. Cole, A new approach to modeling the cure kinetics of epoxy/amine thermosetting resins. 1. Mathematical development, Macromolecules 24 (1991) 3093–3097.
[41] B. Jankovic, The kinetic analysis of isothermal curing reaction of an unsaturated polyester resin: estimation of the density distribution function of the apparent activation energy, Chem. Eng. J. 162 (2010) 331–340.
[42] S. Vyazovkin, N. Sbirrazzuoli, Mechanism and kinetics of epoxy-amine cure studied by differential scanning calorimetry, Macromolecules 29 (1996) 1867–1873.

[43] S. Vyazovkin, N. Sbirrazzuoli, Isoconversional method to explore the mechanism and kinetics of multi-step epoxy cures, Macromol. Rapid Commun. 20 (1999) 387–389.
[44] S. Vyazovkin, N. Sbirrazzuoli, Isoconversional kinetic analysis of thermally stimulated processes in polymers, Macromol. Rapid Commun. 27 (2006) 1515–1532.
[45] H. Stutz, J. Mertes, Influence of the structure on thermoset cure kinetics, J. Polym. Sci. A: Polym. Chem. 31 (1993) 2031–2037.
[46] H. Stutz, J. Mertes, K. Neubecker, Kinetics of thermoset cure and polymerization in the glass transition region, J. Polym. Sci. A: Polym. Chem. 31 (1993) 1879–1886.
[47] T. Takahama, P.H. Geil, The beta relaxation behavior of bisphenol-type resins, J. Polym. Sci. Part B: Polym. Phys. 20 (1982) 1979–1986.
[48] G.W. John, The beta relaxation in epoxy resin-based networks, J. Appl. Polym. Sci. 23 (1979) 3433–3444.
[49] L. Heux, F. Lauprêtre, J.L. Halary, L. Monnerie, Dynamic mechanical and ^{13}C NMR analyses of the effects of antiplasticization on the [beta] secondary relaxation of aryl-aliphatic epoxy resins, Polymer 39 (1998) 1269–1278.
[50] L. Heux, J.L. Halary, F. Lauprêtre, L. Monnerie, Dynamic mechanical and ^{13}C NMR investigations of molecular motions involved in the [beta] relaxation of epoxy networks based on DGEBA and aliphatic amines, Polymer 38 (1997) 1767–1778.
[51] S. Cukierman, J.-L. Halary, L. Monnerie, Dynamic mechanical response of model epoxy networks in the glassy state, Polym. Eng. Sci. 31 (1991) 1476–1482.
[52] J.F. Gerard, J. Galy, J.P. Pascault, S. Cukierman, J.L. Halary, Viscoelastic response of model epoxy networks in the glass transition region, Polym. Eng. Sci. 31 (1991) 615–621.
[53] J.D. LeMay, F.N. Kelley, Structure and ultimate properties of epoxy resins, Adv. Polym. Sci. 78 (1987) 115–148.
[54] S.V. Levchik, E.D. Weil, Thermal decomposition, combustion and flame-retardancy of epoxy resins – a review of the recent literature, Polym. Int. 53 (2004) 1901–1929.